ELSEVIER

Electrical Power and Energy Systems 22 (2000) 543–554

ELECTRICAL POWER & ENERGY SYSTEMS

www.elsevier.com/locate/ijepes

# Pole placement technique for PSS and TCSC-based stabilizer design using simulated annealing

M.A. Abido*

*Electrical Engineering Department, King Fahd University of Petroleum and Minerals, Dhahran 31261, Saudi Arabia*

Received 6 July 1999; revised 14 March 2000; accepted 14 April 2000

**Abstract**

A pole placement technique for power system stabilizer (PSS) and thyristor controlled series capacitor (TCSC) based stabilizer using simulated annealing (SA) algorithm is presented in this paper. The proposed approach employs SA optimization technique to PSS (SAPSS) and TCSC-based stabilizer (SACSC) design. The design problem is formulated as an optimization problem where SA is applied to search for the optimal setting of the proposed SAPSS and SACSC parameters. A pole placement-based objective function to shift the dominant eigenvalues to the left in the *s*-plane is considered. The proposed SAPSS and SACSC have been examined on a weakly connected power system with different disturbances, loading conditions, and system parameter variations. Eigenvalue analysis and nonlinear simulation results show the effectiveness and the robustness of the proposed stabilizers and their ability to provide efficient damping of low frequency oscillations. In addition, the performance of the proposed stabilizers outperforms that of the conventional power system stabilizer (CPSS). It is also observed that the proposed SACSC improves greatly the voltage profile of the system under severe disturbances.


*Keywords*: Thyristor controlled series capacitor; Power system stabilizer; Simulated annealing; Pole placement

## 1. Introduction

Power systems are experiencing low frequency oscillations due to disturbances. The oscillations may sustain and grow to cause system separation if no adequate damping is available. To enhance system damping, the generators are equipped with power system stabilizers (PSSs) that provide supplementary feedback stabilizing signals in the excitation systems. PSSs extend the power system stability limit by enhancing the system damping of low frequency oscillations associated with the electromechanical modes [1].

Eigenvalue assignment techniques have been reported in the literature pertaining to design problems of conventional power system stabilizers (CPSSs) [2,3]. Unfortunately, the proposed techniques are iterative and require heavy computation burden due to system reduction procedure. This gives rise to time consuming computer codes. In addition, the initialization step of these algorithms is crucial and affects the final dynamic response of the controlled system. Hence, different designs assigning the same set of eigenvalues were simply obtained by using different initializations. Therefore, a final selection criterion is required to avoid long runs of validation tests on the nonlinear model. Other techniques such as mathematical programming [4] have been applied to the problem of tuning of PSSs. The problem has been formulated as both a quadratic and a linear programming problem. However, this formulation is carried out at the expense of some conservativeness and the number of constraints becomes unduly large. A gradient procedure for optimization of PSS parameters is presented in [5]. The optimization process requires computations of sensitivity factors and eigenvectors at each iteration. This give rise to heavy computational burdens and slow convergence. In addition, the search process is susceptible to be trapped in local minima and the solution obtained will not be optimal. Several approaches based on modern control theory have been applied to PSS design problem. These include optimal control, adaptive control, variable structure control, and intelligent control [6–9].

The recent advances in power electronics have led to the development of reliable and high-speed flexible AC transmission system (FACTS) devices [10–12] such as static VAR compensator (SVC), thyristor-controlled phase shifter (TCPS), and thyristor controlled series capacitor (TCSC). FACTS are designed to enhance power system stability by increasing the system damping in addition to their primary

* Tel.: +966-3-860-4379; fax: +966-3-860-3535.
*E-mail address:* mabido@kfopm.edu.sa (M.A. Abido).

0142-0615/00/$ - see front matter 
PII: S0142-0615(00)00027-2

**Nomenclature**

| | |
|---|---|
| $P_m$ | Mechanical input power of the generator |
| $P_e$ | Electrical output power of the generator |
| $Z$ | Transmission line impedance, $Z = R + jX$ |
| $Y_L$ | Local load admittance, $Y_L = g + jb$ |
| $D$ | Damping constant of the generator |
| $\delta$ | Rotor angle of the generator |
| $\omega$ | Speed of the generator |
| $\rho$ | Derivative operator d/d$t$ |
| $E_{fd}$ | Field voltage |
| $T'_{do}$ | Open circuit field time constant |
| $x_d$ | $d$-axis reactance of the generator |
| $x'_d$ | $d$-axis transient reactance of the generator |
| $x_q$ | $q$-axis reactance of the generator |
| $K_A$ | Gain of the excitation system |
| $T_A$ | Time constant of the excitation system |
| $V_{ref}$ | Reference voltage |
| $v$ | Terminal voltage of the generator |
| $v_d$ | $d$-axis component of the terminal voltage |
| $v_q$ | $q$-axis component of the terminal voltage |
| $i_d$ | $d$-axis component of the armature current |
| $i_q$ | $q$-axis component of the armature current |
| $E'_q$ | Transient EMF in $q$-axis of the generator |
| $u_{PSS}$ | Output signal of the PSS |
| $u_{CSC}$ | Output signal of the TCSC-based stabilizer |
| $X_{CSC}^{ref}$ | TCSC reference reactance |
| $X_{CSC}$ | TCSC reactance |
| $K_C$ | Gain of the TCSC |
| $T_C$ | Time constant of the TCSC |

functions such as voltage and power flow control. In this paper, the TCSC as one of the promising FACTS devices is considered.

A considerable attention has been directed for investigating the effect of TCSC on power system stability [13–20]. Several approaches based on modern control theory have been applied to TCSC controller design. Chen et al. [13] presented a state feedback controller for TCSC by using a pole placement technique. However, the controller requires all system states. This reduces its applicability. Chang and Chow [14] developed a time optimal control strategy for the TCSC where a performance index of time was minimized. A fuzzy logic controller for a TCSC was proposed in [15]. The impedance of the TCSC was adjusted based on machine rotor angle and the magnitude of the speed deviation. In addition, different control schemes for a TCSC were proposed such as variable structure controller [16,17], bilinear generalized predictive controller [18], $H_\infty$-based controller [19], and neural network controller [20].

Despite the potential of modern control techniques with different structures, power system utilities still prefer a conventional lead-lag controller structure [21–23]. The reasons behind that might be the ease of on-line tuning and the lack of assurance of the stability related to some adaptive or variable structure techniques. It is shown that the appropriate selection of conventional lead-lag stabilizer parameters results in effective damping to low frequency oscillations [23].

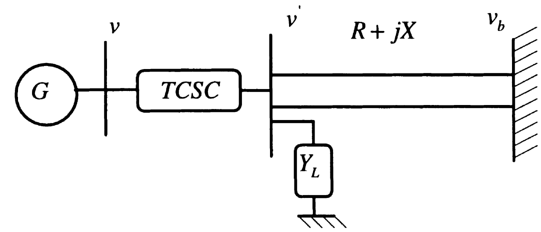


Fig. 1. Single machine infinite bus system with a TCSC.

In the last few years, simulated annealing (SA) algorithm [24–26] appeared as a promising heuristic algorithm for handling the combinatorial optimization problems. It has been theoretically proved that the SA algorithm converges to the optimum solution. The SA algorithm is robust, i.e. the final solution quality does not strongly depend on the choice of the initial solution. Therefore, the algorithm can be used to improve the solution of other methods. Another strong feature of SA algorithm is that a complicated mathematical model is not required and the constraints can be easily incorporated [24]. Unlike the gradient-descent techniques, SA is a derivative-free optimization algorithm and no sensitivity analysis is required to evaluate the objective function. This feature simplifies the constraints imposed on the objective function considered.

In this paper, a pole placement technique for simulated annealing-based PSS (SAPSS) and simulated annealing-based TCSC stabilizer (SACSC) design is presented. The design objective is to shift the unstable and poorly damped modes to the left in the $s$-plane. The proposed SAPSS and SACSC have been applied and tested on a weakly connected power system under several loading conditions and severe disturbances. The effectiveness of the proposed stabilizers to extend the system stability limit and to improve the system voltage profile is demonstrated. In addition, the robustness of the proposed stabilizers to system parameter variations is examined.

## 2. Thyristor controlled series capacitor

In this study, a single machine infinite bus system with a TCSC shown in Fig. 1 is considered. A TCSC has been placed in series with the transmission line to change the line flow. Therefore, a TCSC can extend the power transfer capability and provide additional damping for low frequency oscillations. The configuration of a TCSC is shown in Fig. 2. It comprises a fixed capacitor in parallel with a thyristor-controlled reactor. Controlling the firing angle of the thyristors can regulate the TCSC reactance and its degree of compensation.

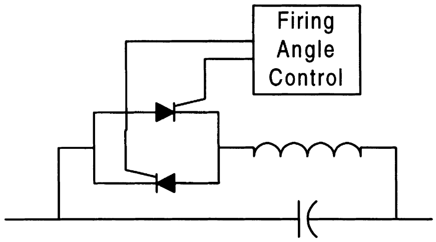


Fig. 2. The configuration of TCSC.

## 3. Linearized power system model

The generator is represented by the third-order model comprising of the electromechanical swing equation and the generator internal voltage equation. The swing equation is divided into the following equations:

$$\rho\delta = \omega_b(\omega - 1) \tag{1}$$

$$\rho\omega = \frac{(P_m - P_e - D)(\omega - 1))}{M} \tag{2}$$

$P_m$ is assumed to be constant and $P_e$ can be expressed as

$$P_e = v_d i_d + v_q i_q \tag{3}$$

The internal voltage, $E'_q$, equation is

$$\rho E'_q = \frac{(E_{fd} - (x_d - x'_d)i_d - E'_q)}{T'_{do}} \tag{4}$$

The IEEE Type-ST1 excitation system shown in Fig. 3 is considered in this study. It can be described as

$$\rho E_{fd} = \frac{(K_A(V_{ref} - v + u_{PSS}) - E_{fd})}{T_A} \tag{5}$$

where

$$v = (v_d^2 + v_q^2)^{1/2} \tag{6}$$

$$v_d = x_q i_q \tag{7}$$

$$v_q = E'_q - x'_d i_d \tag{8}$$

Fig. 4 illustrates the block diagram of a TCSC with conventional lead-lag stabilizer. The TCSC dynamics can be expressed as

$$\rho X_{CSC} = \frac{(K_c(X_{CSC}^{ref} + u_{CSC}) - X_{CSC})}{T_c} \tag{9}$$

where $X_{CSC}^{ref}$ represents the desired degree of compensation.

In the design of damping controller, the linearized incremental model around a nominal operating point is usually employed [1]. The linearized power system model can be written as, see Appendix A,

$$\begin{bmatrix} \rho\Delta\delta \\ \rho\Delta\omega \\ \rho\Delta E'_q \\ \rho\Delta E_{fd} \end{bmatrix} = \begin{bmatrix} 0 & 377 & 0 & 0 \\ -\frac{K_1}{M} & -\frac{D}{M} & -\frac{K_2}{M} & 0 \\ -\frac{K_4}{T'_{do}} & 0 & -\frac{K_3}{T'_{do}} & \frac{1}{T'_{do}} \\ -\frac{K_A K_5}{T_A} & 0 & -\frac{K_A K_6}{T_A} & -\frac{1}{T_A} \end{bmatrix} \times \begin{bmatrix} \Delta\delta \\ \Delta\omega \\ \Delta E'_q \\ \Delta E_{fd} \end{bmatrix} + \begin{bmatrix} 0 & 0 \\ 0 & -\frac{K_p}{M} \\ 0 & -\frac{K_q}{T'_{do}} \\ \frac{K_A}{T_A} & -\frac{K_A K_v}{T_A} \end{bmatrix} \begin{bmatrix} u_{PSS} \\ \Delta X_{CSC} \end{bmatrix} \tag{10}$$

In short, the linearized system model can be written as

$$\rho X = AX + BU \tag{11}$$

Fig. 5 illustrates the block diagram of the linearized power system model. The expressions of constants $K_1 - K_6$, $K_p$, $K_q$, and $K_v$ are given in Appendix A.

## 4. Simulated annealing algorithm

### 4.1. Overview

Simulated annealing is an optimization technique that simulates the physical annealing process in the field of combinatorial optimization. Annealing is the physical

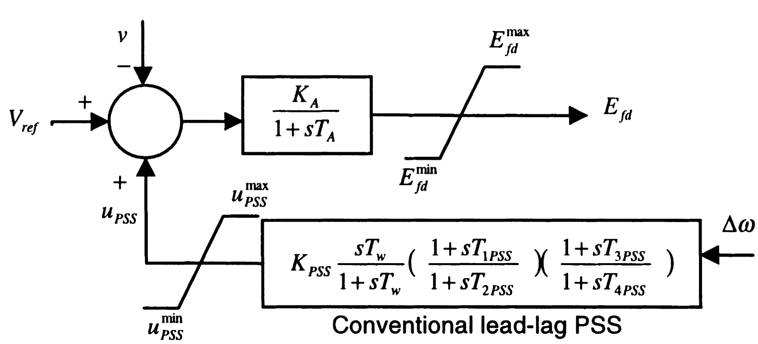


Fig. 3. IEEE Type-ST1 excitation system with conventional PSS.

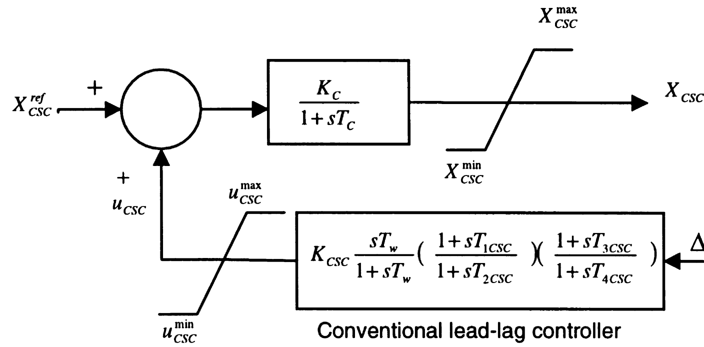


Fig. 4. TCSC with conventional lead-lag stabilizer.

process of heating up a solid until it melts, followed by slow cooling it down by decreasing the temperature of the environment in steps. At each step, the temperature is maintained constant for a period of time sufficient for the solid to reach thermal equilibrium. At any temperature $T$, the thermal equilibrium state is characterized by the *Boltzmann distribution*. This distribution gives the probability of the solid being in a state $i$ with energy $E_i$ at temperature $T$ as

$$P_i = k\exp(-E_i/T) \tag{12}$$

where $k$ is a constant.

Metropolis et al. [25] proposed a Monte Carlo method to simulate the process of reaching thermal equilibrium at a fixed value of the temperature $T$. In this method, a randomly generated perturbation of the current configuration of the solid is applied so that a trial configuration is obtained. Let $E_c$ and $E_t$ denote the energy level of the current and trial configurations, respectively. If $E_t < E_c$, then a lower energy level has been reached, and the trial configuration is accepted and becomes the current configuration. On the other hand, if $E_t \geq E_c$ the trial configuration is accepted as current configuration with probability proportional to $\exp(-\Delta E/T)$, $\Delta E = E_t - E_c$. The process continues until the thermal equilibrium is achieved after a large number of perturbations, where the probability of a configuration approaches the *Boltzmann distribution.*

By gradually decreasing the temperature $T$ and repeating Metropolis simulation, new lower energy levels become achievable. As $T$ approaches *zero* least energy configurations will have a positive probability of occurring.

### 4.2. SA algorithm

At first, the analogy between a physical annealing process and a combinatorial optimization problem is based on the following [24]:

- Solutions in an optimization problem are equivalent to configurations of a physical system.
- The cost of a solution is equivalent to the energy of a configuration.

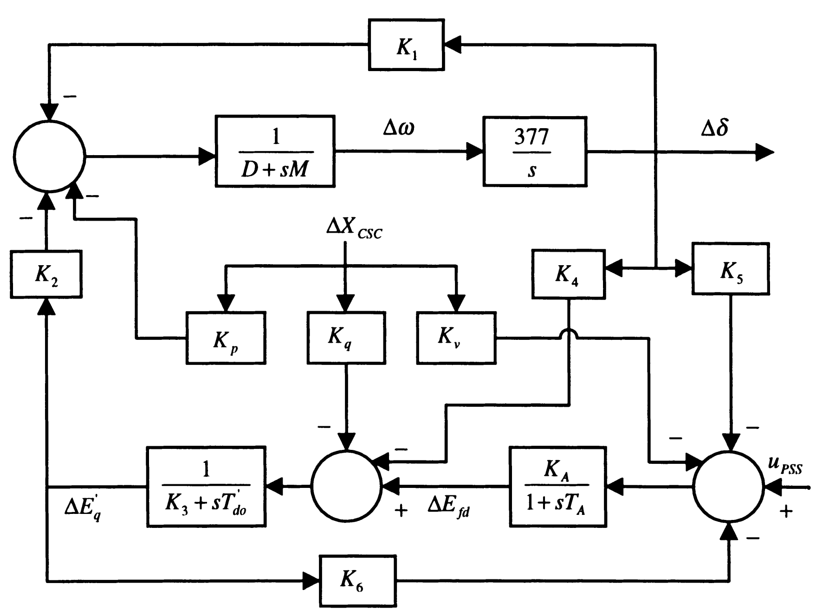


Fig. 5. Block diagram of the linearized power system model.

In addition, a control parameter $C_p$ is introduced to play the role of the temperature $T$.

The basic elements of SA are briefly stated and defined as follows.

- *Current, trial, and best solutions*, $x_{current}$, $x_{trial}$, and $x_{best}$: these solutions are sets of the optimized parameter values at any iteration.
- *Acceptance criterion:* at any iteration, the trial solution can be accepted as the current solution if it meets one of the following critera—(a) $J(x_{trial}) < J(x_{current})$; (b) $J(x_{trial}) > J(x_{current})$ and $\exp(-(J(x_{trial}) - J(x_{current}))/C_p) \geq \mathrm{rand}(0,1)$. Here, rand(0,1) is a random number with domain [0,1] and $J(x_{trial})$ and $J(x_{current})$ are the objective function values associated with $x_{trial}$ and $x_{current}$, respectively. Criterion (b) indicates that the trial solution is not necessarily rejected if its objective function is not as good as that of the current solution with hoping that a much better solution becomes reachable.
- *Acceptance ratio:* at a given value of $C_p$, an $n_1$ trial solutions can be randomly generated. Based on the acceptance criterion, an $n_2$ of these solutions can be accepted. The acceptance ratio is defined as $n_2/n_1$.
- *Markov chain:* it is defined as a sequence of trial solutions where the probability of the outcome of a given trial solution depends only on the outcome of the previous trial solution. In the SA algorithm, the set of the outcomes is given by the finite set of solutions. The acceptance criteria described above show clearly that the outcome of a trial solution depends only on the outcome of the previous one. Hence, the concept of the Markov chain can be used [24]. The allowable number of transitions at each value of the control parameter $C_p$ represents the length of each chain.
- *Cooling schedule:* it specifies a set of parameters that governs the convergence of the algorithm. This set includes an initial value of control parameter $C_{p0}$, a decrement function for decreasing the value of $C_p$, and a finite number of iterations or transitions at each value of $C_p$, i.e. the length of each homogeneous Markov chain. The initial value of $C_p$ should be large enough to allow virtually all transitions to be accepted. However, this can be achieved by starting off at a small value of $C_{p0}$ and multiplying it with a constant larger than 1, $\alpha$, i.e. $C_{p0} = \alpha C_{p0}$. This process continues until the acceptance ratio is close to 1. This is equivalent to heating up process in physical systems. The decrement function for decreasing the value of $C_p$ is given by $C_p = \mu C_p$ where $\mu$ is a constant smaller than but close to 1. Typical values lie between 0.8 and 0.99 [24]. The acceptance criteria show that at large values of $C_p$, large deteriorations will be accepted; as $C_p$ decreases, only smaller deteriorations will be accepted and finally, as $C_p$ approaches *zero*, no deteriorations will be accepted at all. This feature, in contrast to gradient-descent and other local search algorithms, avoids trapping in local minima.
- *Equilibrium condition:* it occurs when the current solution does not change for a certain number of iterations at a given value of $C_p$. It can be achieved by generating a large number of transitions at that value of $C_p$.
- *Stopping criteria:* these are the conditions under which the search process will terminate. In this study, the search will terminate if one of the following criteria is satisfied—(a) the number of Markov chains since the last change of the best solution is greater than a prespecified number; or (b) the number of Markov chains reaches the maximum allowable number.

The general algorithm of SA can be described in steps as follows.

*Step 1:*Set the initial value of $C_{p0}$ and randomly generate an initial solution $x_{initial}$ and calculate its objective function. Set this solution as the current solution as well as the best solution, i.e. $x_{initial} = x_{current} = x_{best}$.
*Step 2:*Randomly generate an $n_1$ of trial solutions in the neighborhood of the current solution.
*Step 3:*Check the acceptance criterion of these trial solutions and calculate the acceptance ratio. If acceptance ratio is close to 1 go to step 4; else set $C_{p0} = \alpha C_{p0},\ \alpha > 1$, and go back to Step 2.
*Step 4:*Set the chain counter $k_{ch} = 0$.
*Step 5:*Generate a trial solution $x_{trial}$. If $x_{trial}$ satisfies the acceptance criterion set $x_{current} = x_{trial}$, $J(x_{current}) = J(x_{trial})$, and go to Step 6; else go to Step 6.
*Step 6:*Check the equilibrium condition. If it is satisfied go to Step 7; else go to Step 5.
*Step 7:*Check the stopping criteria. If one of them is satisfied then stop; else set $k_{ch} = k_{ch} + 1$ and $C_p = \mu C_p,\ \mu < 1$, and go back to Step 5.

## 5. Proposed design approach

### 5.1. Structure of the proposed stabilizers

A conventional lead-lag controller structure for both SAPSS and SACSC as shown in Figs. 2 and 3 is considered in this study. The stabilizing signals of the proposed SAPSS and SACSC can be expressed as

$$u_{PSS} = K_{PSS}\frac{sT_w}{1+sT_w}\left(\frac{1+sT_{1\,PSS}}{1+sT_{2\,PSS}}\right)\left(\frac{1+sT_{3\,PSS}}{1+sT_{4\,PSS}}\right)\Delta\omega \quad (13)$$

$$u_{CSC} = K_{CSC}\frac{sT_w}{1+sT_w}\left(\frac{1+sT_{1\,CSC}}{1+sT_{2\,CSC}}\right)\left(\frac{1+sT_{3\,CSC}}{1+sT_{4\,CSC}}\right)\Delta\omega \quad (14)$$

In this structure, the washout time constant $T_w$ and the time constants $T_{2\,PSS}$, $T_{4\,PSS}$, $T_{2\,CSC}$, and $T_{4\,CSC}$ are usually prespecified. In this study, $T_w = 5$ s and $T_{2\,PSS} = T_{4\,PSS} = T_{2\,CSC} = T_{4\,CSC} = 0.1$ s. The controller gains, $K_{PSS}$ and

$K_{CSC}$, and time constants, $T_{1\ PSS}$, $T_{3\ PSS}$, $T_{1\ CSC}$, and $T_{3\ CSC}$ remain to be determined.

### *5.2. Problem formulation*

To increase the system damping to the electromechanical modes, the objective function $J$ defined below is proposed.

$$J = \sum_{\sigma_i \geq \sigma_0} (\sigma_0 - \sigma_i)^2 \quad (15)$$

where $\sigma_i$ is the real part of the $i^{th}$ eigenvalue and $\sigma_0$ is a chosen threshold. The value of $\sigma_0$ represents the desirable level of system damping. This level can be achieved by shifting the dominant eigenvalues to the left of $s = \sigma_0$ line in the $s$-plane. This insures also some degree of relative stability. The condition $\sigma_i \geq \sigma_0$ is imposed on $J$ evaluation to consider only the unstable or poorly damped modes.

The problem constraints are the parameter bounds. Therefore, the design problem can be formulated as the following optimization problem.

$$\text{Minimize } J \quad (16)$$

Subject to

$$K_{PSS}^{min} \leq K_{PSS} \leq K_{PSS}^{max} \quad (17)$$

$$T_{1\ PSS}^{min} \leq T_{1\ PSS} \leq T_{1\ PSS}^{max} \quad (18)$$

$$T_{3\ PSS}^{min} \leq T_{3\ PSS} \leq T_{3\ PSS}^{max} \quad (19)$$

$$K_{CSC}^{min} \leq K_{CSC} \leq K_{CSC}^{max} \quad (20)$$

$$T_{1\ CSC}^{min} \leq T_{1\ CSC} \leq T_{1\ CSC}^{max} \quad (21)$$

$$T_{3\ CSC}^{min} \leq T_{3\ CSC} \leq T_{3\ CSC}^{max} \quad (22)$$

The minimum and maximum values of the controller gains are set as 0.1 and 100, respectively [26]. The minimum values of $T_{1\ PSS}$ and $T_{3\ PSS}$ are set slightly above the value of $T_{2\ PSS}$ and $T_{4\ PSS}$, respectively, to compensate the phase lag between $u_{PSS}$ and $E'_q$ [27]. The maximum values of $T_{1\ PSS}$, $T_{3\ PSS}$, $T_{1\ CSC}$, and $T_{3\ CSC}$ are set to 1.0 s.

Table 1
The optimal settings of the controller parameters of the proposed schemes

| Proposed SAPSS | | | Proposed SACSC | | |
|---|---|---|---|---|---|
| $K_{PSS}$ | $T_{1\ PSS}$ | $T_{3\ PSS}$ | $K_{CSC}$ | $T_{1\ CSC}$ | $T_{3\ CSC}$ |
| 22.523 | 0.1212 | 0.2156 | 74.726 | 0.0115 | 0.1249 |

### *5.3. Application of SA algorithm*

The SA algorithm has been applied to the above optimization problem to search for optimal settings of the proposed stabilizers. In our implementation, the threshold value $\sigma_0$ was chosen to be $-3.0$. The search will terminate if one of the following stopping criteria is satisfied: (1) best solution does not change for more than 20 chains; (2) number of chains reaches 100; or (3) value of the objective function reaches *zero*, i.e. all the dominant eigenvalues have been shifted to the left of $s = \sigma_0$ line.

The final settings of the optimized parameters for the proposed stabilizers are given in Table 1. The convergence rate of the objective function $J$ with the number of iterations is shown in Fig. 6. It is worth mentioning that the optimization process has been carried out with the system operating at nominal loading condition given in Table 2.

## 6. Simulation results

To assess the effectiveness and robustness of the proposed stabilizers, three different loading conditions given in Table 2 were considered with different

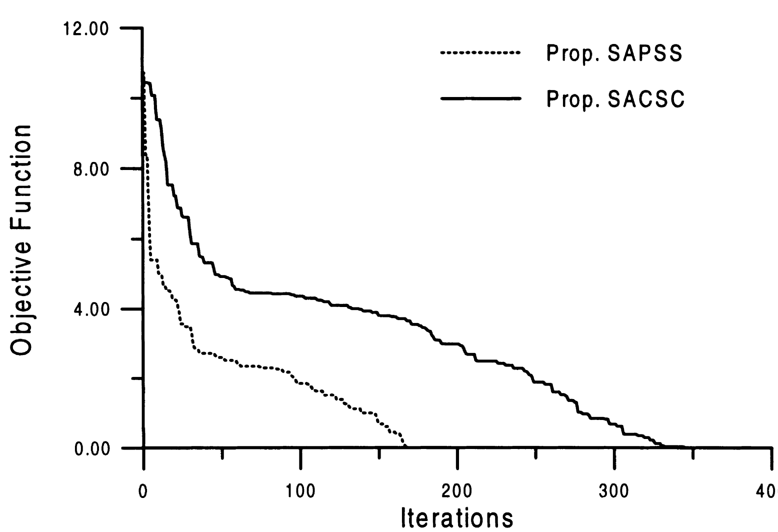


Fig. 6. Objective function variations of the proposed schemes.

Table 2
Loading conditions

| Loading | $P$ (pu) | $Q$ (pu) | $X_{CSC}$ (pu) |
|---|---|---|---|
| Nominal | 1.00 | 0.015 | 0.0 |
| Light | 0.70 | 0.300 | 0.2 |
| Heavy | 1.10 | 0.400 | −0.2 |

Table 3
System eigenvalues with and without control in 1/s

| No Control | CPSS | Prop. SAPSS | Prop. SACSC |
|---|---|---|---|
| $+0.30 \pm j4.96$ | $-1.16 \pm j4.40$ | $-3.00 \pm j6.74$ | $-3.32 \pm j5.57$ |
| $-10.39 \pm j3.28$ | $-4.60 \pm j7.41$ | $-3.29 \pm j4.67$ | $-4.31 \pm j5.77$ |
| – | −0.20, −18.68 | −19.24, −8.37 | −13.47, −8.37 |
| – | – | −0.21 | −23.09, −0.21 |

disturbances. The performance of the proposed stabilizers is compared to that of CPSS given in Refs. [27,28].

It is worth mentioning that all the time domain simulations were carried out using the nonlinear power system model. The system data is given in Appendix A.

### 6.1. Nominal loading

At this loading condition, the system eigenvalues with and without the proposed stabilizers are given in Table 3. It is shown that the open loop system is unstable because of the negative damping of electromechanical mode. It is quite clear that the proposed stabilizers outperform the CPSS and shift substantially the electromechanical mode eigenvalue to the left of the line $s = -3.0$ in the $s$-plane. This enhances greatly the system stability and improves the damping characteristics of electromechanical mode.

The behavior of the proposed stabilizer under transient conditions was verified by applying a 6-cycle three-phase fault at the infinite bus at the end of one transmission line. The fault was cleared without line tripping. The system response is shown in Fig. 7. It can be seen that the response

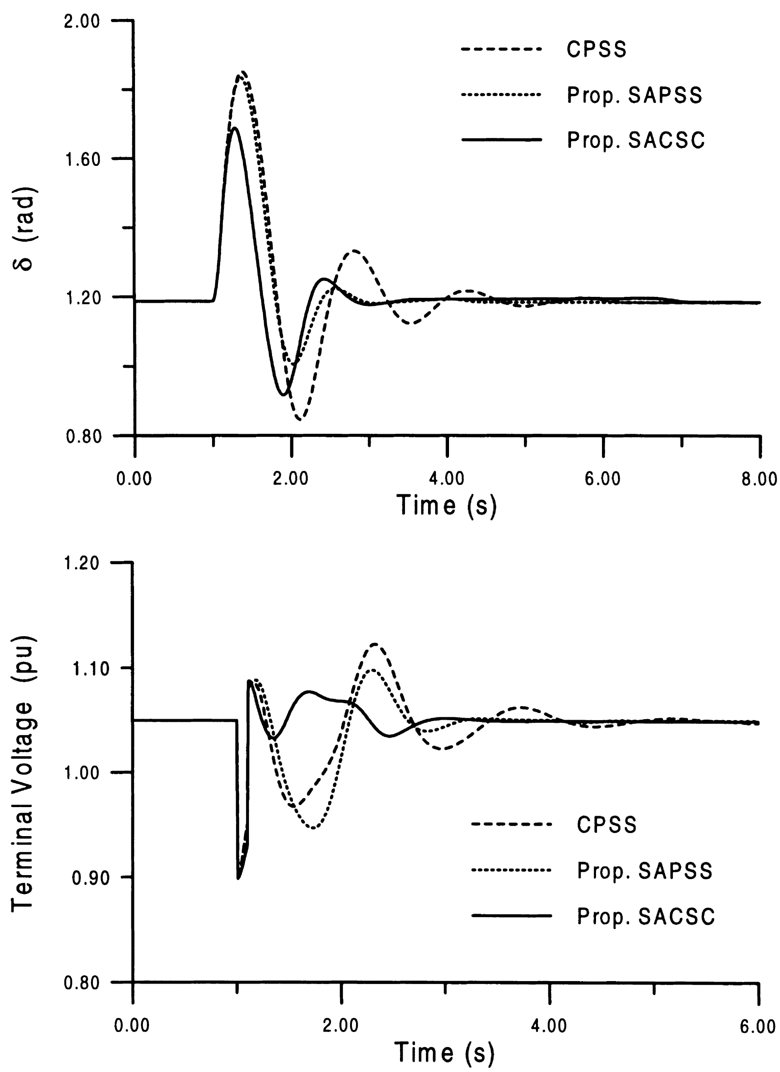


Fig. 7. System response to the fault test with nominal loading without line tripping.

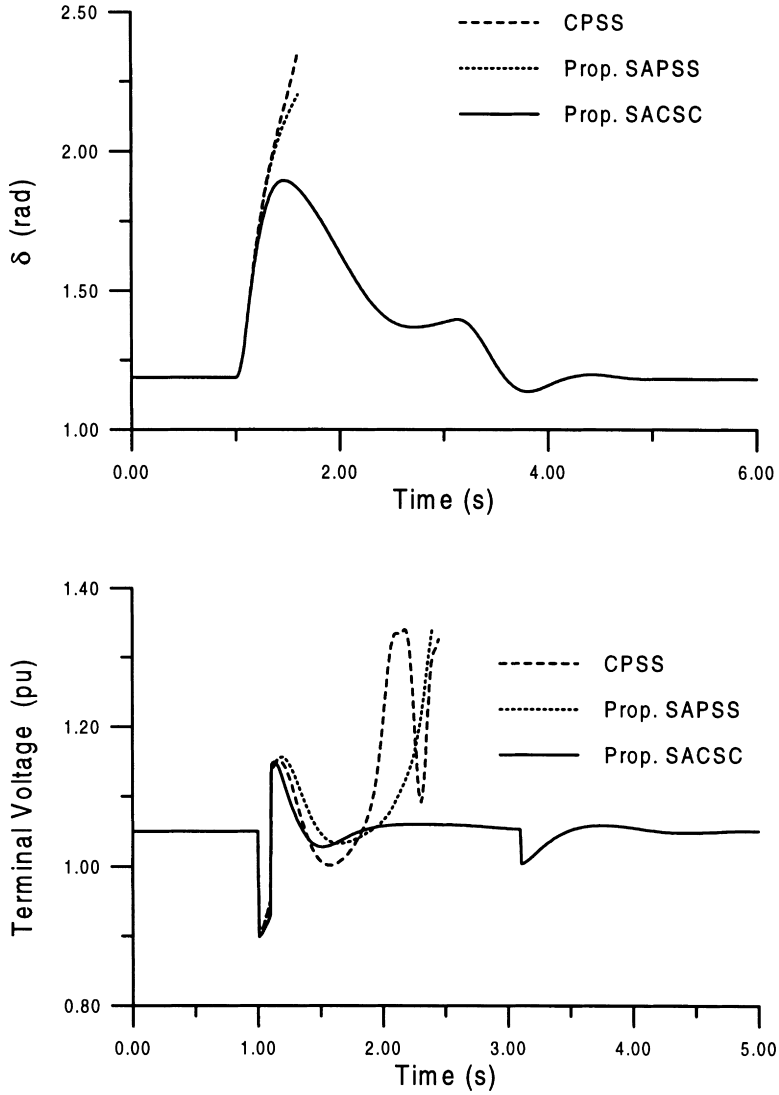


Fig. 8. System response to the fault test with nominal loading with line tripping for 2 s.

of the proposed stabilizers is much faster than that of CPSS. In addition, the first swing in the torque angle is significantly suppressed and the voltage profile is greatly improved with the proposed SACSC.

Another severe disturbance was considered at this loading condition; that is, a 6-cycle fault was applied as above. However, the faulty line was tripped for 2 s. The system response to this disturbance is shown in Fig. 8. It is clear that the proposed SACSC has good damping characteristics to low frequency oscillations and stabilizes the system under this severe disturbance. This extends the power system stability limit and the power transfer capability. These positive results of the proposed SACSC can be attributed to its faster response compared to that of power system stabilizer. It can be concluded that although PSSs extend the power system stability limit by enhancing the system damping, they suffer a drawback of being liable to cause great variations in the voltage profile and they may even result in losing system stability under severe disturbances.

### 6.2. Light loading

A 6-cycle three-phase fault disturbance at the infinite bus was applied. The faulty line was tripped for 4 s. The results are shown in Fig. 9. It can be seen that the proposed stabilizers suppress the first swing in torque angle and extend the system stability limit. In addition, the voltage profile is greatly improved with the proposed SACSC stabilizer in terms of overshoots and settling time.

A parameter variation test was also applied to assess the robustness of the proposed stabilizers. At $t = 1$ s, one of the transmission lines was tripped for maintenance purposes, i.e. the line impedance was doubled. The system response is shown in Fig. 10. It is clear that the proposed stabilizers outperform the CPSS. In addition, the system

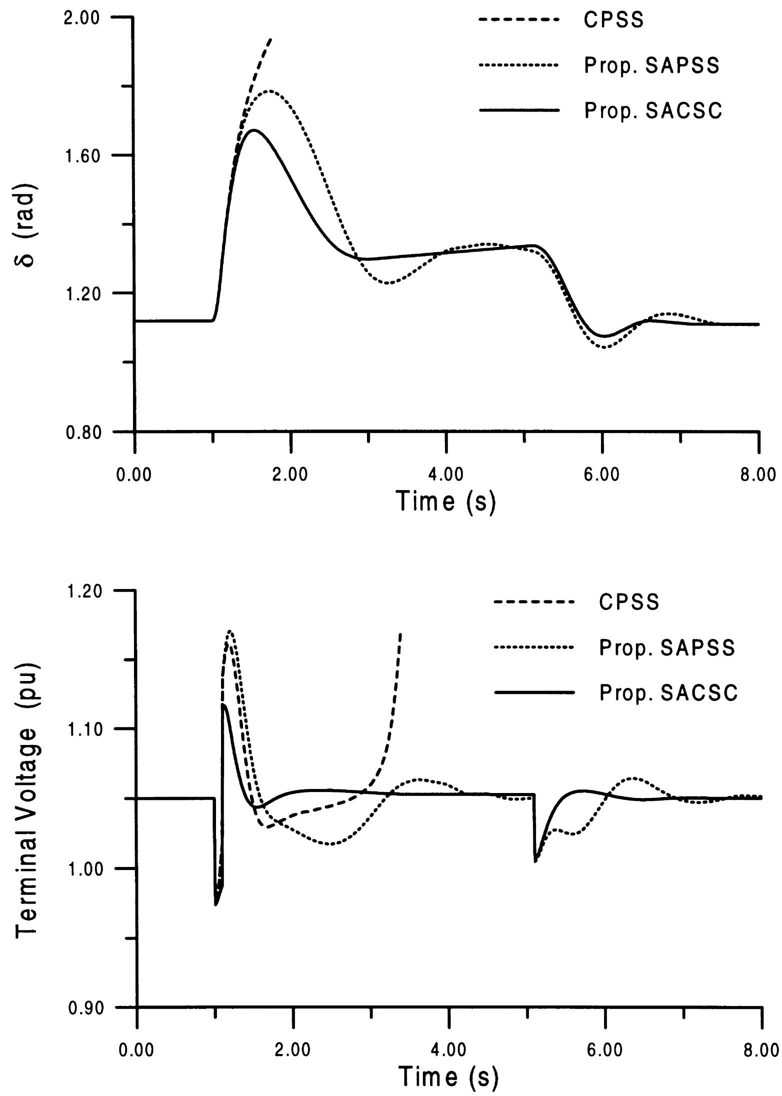


Fig. 9. System response to the fault test with light loading with line tripping for 4 s.

voltage profile is greatly improved with the proposed SACSC.

### 6.3. Heavy loading

A 5-cycle three-phase fault disturbance at the infinite bus was applied. The results are shown in Fig. 11. It can be seen that the first swing is substantially suppressed and the voltage profile is greatly improved with the proposed SACSC. It can be concluded that the proposed SACSC has better damping characteristics to electromechanical modes of oscillations and improves greatly the power system stability and system voltage profile.

## 7. Conclusions

In this study, a pole placement technique for PSS and TCSC-based stabilizer is presented. The tuning parameters of the proposed SAPSS and SACSC were optimized using simulated annealing algorithm as the optimization engine. The proposed stabilizers have been applied and tested on a weakly connected power system under different disturbances, loading conditions, and system parameter variations. The eigenvalue analysis and the nonlinear simulation results show the effectiveness and the robustness of the proposed stabilizers and their ability to provide good damping of low frequency oscillations and improve greatly the system voltage profile. In addition, the TCSC-based stabilizer outperforms the power system stabilizers in terms of the first swing stability and the voltage profile. It can be concluded that although PSSs extend the power system stability limit by enhancing the system damping, they suffer a drawback of being liable to cause great variations in the voltage profile and they may even result in losing system stability under severe disturbances.

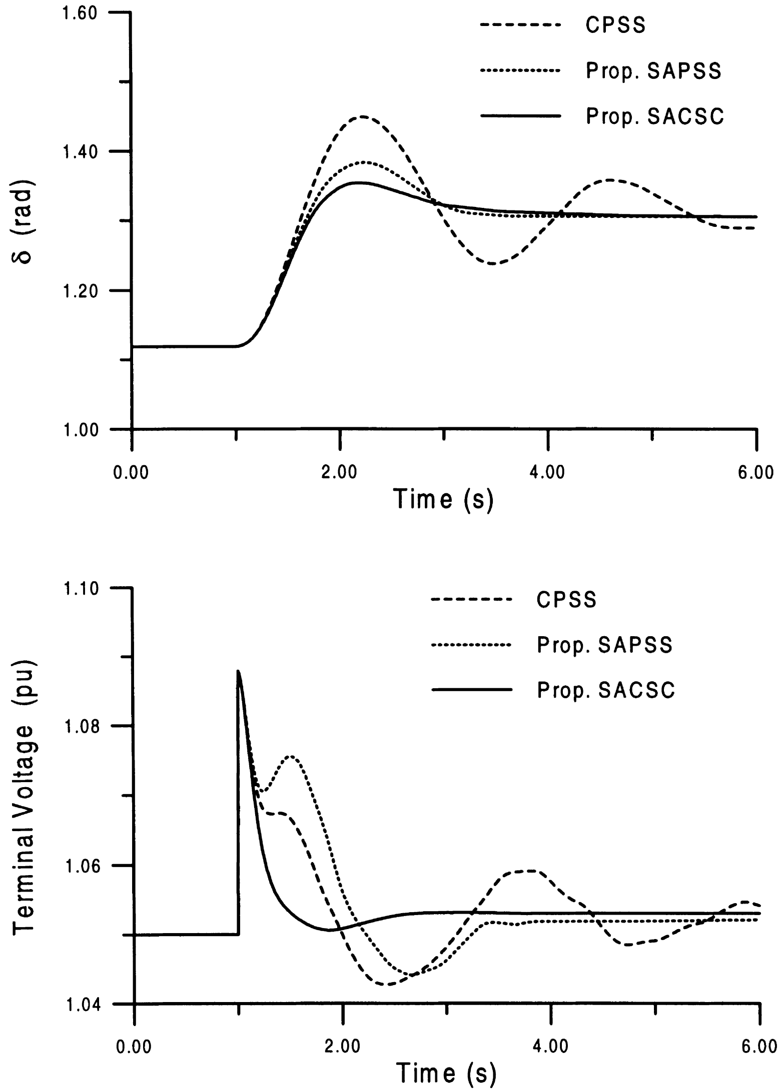


Fig. 10. System response to the line impedance variation test with light loading.

## Acknowledgements

The author acknowledges the support of King Fahd University of Petroleum & Minerals, Saudi Arabia.

## Appendix A

Referring to Fig. 1, the voltage $v' = v - jX_{\mathrm{CSC}}i$, $i$ is the generator armature current. The $d$ and $q$ components of $v'$ can be written as

$$v'_d = (x_q + X_{\mathrm{CSC}})i_q \tag{A1}$$

$$v'_q = E'_q - (x'_d + X_{\mathrm{CSC}})i_d \tag{A2}$$

The load current $i_{\mathrm{L}} = v'Y_{\mathrm{L}}$, and the line current $i_{\mathrm{line}} = i - i_{\mathrm{L}}$. The infinite bus voltage $v_{\mathrm{b}} = v' - i_{\mathrm{line}}Z$. The components of $v_{\mathrm{b}}$ can be written as

$$v_{\mathrm{b}} \sin\delta = c_1 v'_d - c_2 v'_q - Ri_d + Xi_q \tag{A3}$$

$$v_{\mathrm{b}} \cos\delta = c_2 v'_d + c_1 v'_q - Xi_d - Ri_q \tag{A4}$$

Substituting from Eqs. (A1) and (A2) into Eqs. (A3) and (A4), the following two equations can be obtained:

$$c_3 i_d + c_4 i_q = v_b \sin\delta + c_2 E'_q \tag{A5}$$

$$c_5 i_d + c_6 i_q = v_{\mathrm{b}} \cos\delta - c_1 E'_q \tag{A6}$$

Solving Eqs. (A5) and (A6) simultaneously, $i_d$ and $i_q$ expressions can be obtained. Linearizing Eqs. (A5) and (A6) at the nominal loading condition, $\Delta i_d$ and $\Delta i_q$ can be expressed in

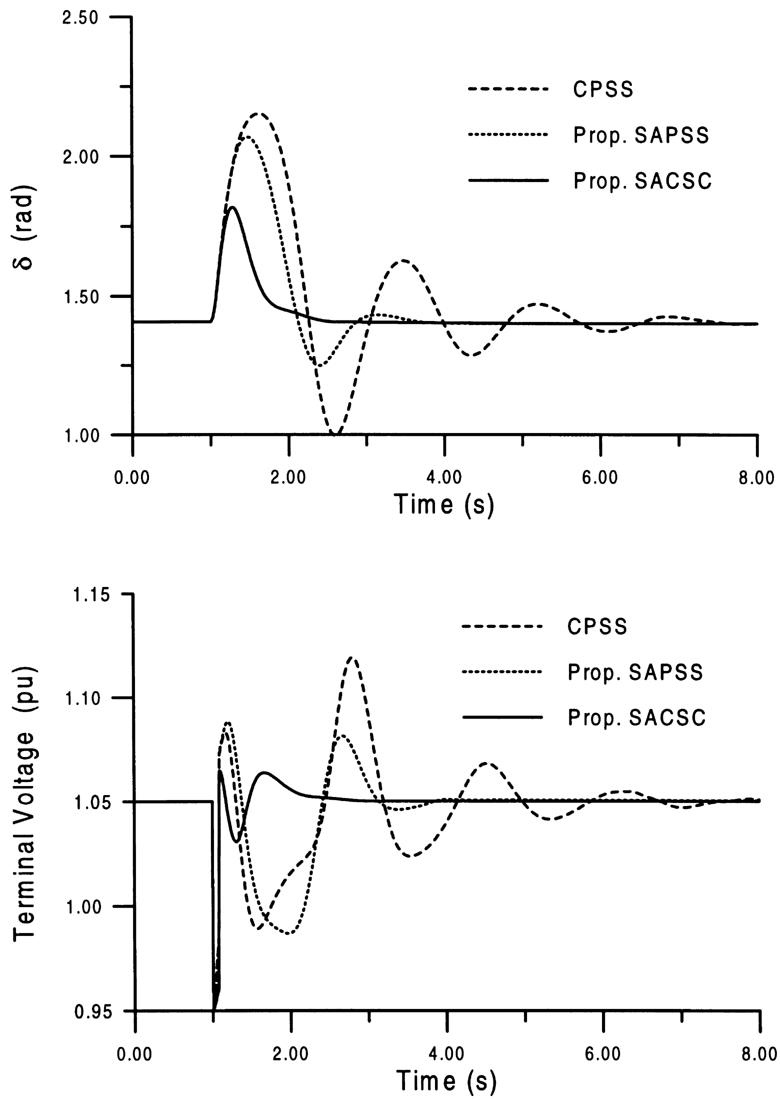


Fig. 11. System response to the fault test with heavy loading.

terms of $\Delta\delta$, $\Delta E'_q$, and $\Delta X_{\mathrm{CSC}}$ as follows:

$$c_3\Delta i_d + c_4\Delta i_q = v_{\mathrm{b}} \cos \delta\Delta\delta + c_2\Delta E'_q + c_7\Delta X_{\mathrm{CSC}} \quad \text{(A7)}$$

$$c_5\Delta i_d + c_6\Delta i_q = -v_{\mathrm{b}} \sin \delta\Delta\delta - c_1\Delta E'_q + c_8\Delta X_{\mathrm{CSC}} \quad \text{(A8)}$$

Solving Eqs. (A7) and (A8) simultaneously, $\Delta i_d$ and $\Delta i_q$ can be expressed as

$$\Delta i_d = c_9\Delta\delta + c_{10}\Delta E'_q + c_{11}\Delta X_{\mathrm{CSC}} \quad \text{(A9)}$$

$$\Delta i_q = c_{12}\Delta\delta + c_{13}\Delta E'_q + c_{14}\Delta X_{\mathrm{CSC}} \quad \text{(A10)}$$

The constants $c_1$–$c_{14}$ are expressions of $Z, Y_{\mathrm{L}}, x'_d, x_q$, $i_{d0}, i_{qo}, E'_{q0}$, and $X_{\mathrm{CSC}}$

The linearized form of $v_d$ and $v_q$ can be written as

$$\Delta v_d = x_q\Delta i_q \quad \text{(A11)}$$

$$\Delta v_q = \Delta E'_q - x'_d\Delta i_d \quad \text{(A12)}$$

Using Eqs. (A1)–(A12),, the following expressions can be easily obtained

$$\Delta P_{\mathrm{e}} = K_1\Delta\delta + K_2\Delta E'_q + K_{\mathrm{p}}\Delta X_{\mathrm{CSC}} \quad \text{(A13)}$$

$$(K_3 + sT'_{\mathrm{do}})\Delta E'_q = \Delta E_{\mathrm{fd}} - K_4\Delta\delta - K_q\Delta X_{\mathrm{CSC}} \quad \text{(A14)}$$

$$\Delta v = K_5\Delta\delta + K_6\Delta E'_q + K_v\Delta X_{\mathrm{CSC}} \quad \text{(A15)}$$

where the constants $K_1$–$K_6$, $K_p$, $K_q$, and $K_v$ are expressions of $c_9$–$c_{14}$.

## Appendix B

The system data are as follows.

$M = 9.26$ s; $T'_{\mathrm{do}} = 7.76$; $D = 0.0$;

$x_d = 0.973$; $x'_d = 0.19$; $x_q = 0.55$;

$R = -0.034;$[1] $\quad X = 0.997; \quad g = 0.249;$

$b = 0.262; \quad K_A = 50; \quad T_A = 0.05;$

$K_s = 1.0; \quad T_s = 0.05;$

$|u_{PSS}| \le 0.2$ pu; $|u_{CSC}| \le 0.2$ pu;

$|X_{CSC}| = 0.5X|E_{fd}| \le 7.3$ pu.

All resistances and reactances are in pu and time constants are in seconds.

With the nominal loading condition given in Table 2, the system matrices are

$$A = \begin{bmatrix} 0.0 & 3.77 & 0.0 & 0.0 \\ -0.0588 & 0.0 & -0.1303 & 0.0 \\ -0.0900 & 0.0 & -0.1957 & 0.1289 \\ 95.5320 & 0.0 & -815.93 & -20.00 \end{bmatrix}$$

$$B = \begin{bmatrix} 0.0 & 0.0 \\ 0.0 & 0.0704 \\ 0.0 & 0.0177 \\ 1000 & 93.846 \end{bmatrix}$$

## References


[1] deMello FP, Concordia C. Concepts of synchronous machine stability as affected by excitation control. IEEE Trans PAS 1969;88:316–29.

[2] Lim CM, Elangovan S. Design of stabilizers in multimachine power systems. IEE Proc C 1985;132(3):146–53.

[3] Yu YN, Li Q. Pole-placement power system stabilizers design of an unstable nine-machine system. IEEE Trans PWRS 1990;5(2):353–8.

[4] da Cruz JJ, Zanetta LC. Stabilizer design for multimachine power systems using mathematical programming. Int J Electrical Power and Energy Syst 1997;19(8):519–23.

[5] Maslennikov VA, Ustinov SM. The optimization method for coordinated tuning of power system regulators. Proceedings of the 12th Power System Computation Conference PSCC, Dresden, 1996. p. 70–5.

[6] Osheba SM, Hogg BW. Performance of state space controllers for turbogenerators in multimachine power systems. IEEE Trans PAS 1982;101(9):3276–83.

[7] Xia D, Heydt GT. Self-tuning controller for generator excitation control. IEEE Trans PAS 1983;102:1877–85.

[8] Samarasinghe V, Pahalawaththa N. Damping of multimodal oscillations in power systems using variable structure control techniques. IEE Proc Genet Trans Distrib 1997;144(3):323–31.

[9] Abido MA, Abdel-Magid YL. Hybridizing rule-based power system stabilizers with genetic algorithms. IEEE Trans Power Syst 1999;14(2):600–7.

[10] Noroozian M, Anderson G. Power flow control by use of controllable series components. IEEE Trans Power Delivery 1993;8(3):1420–9.

[11] Rahim A, Nassimi S. Synchronous generator damping enhancement through coordinated control of exciter and SVC. IEE Proc Genet Trans Distrib 1996;143(2):211–8.

[12] Mahran A, Hogg B, Al-Sayed ML. Coordinated control of synchronous generator excitation and static VAR compensator. IEEE Trans Energy Conversion 1992;7(4):615–22.

[13] Chen X, Pahalawaththa N, Annakkage U, Kumble C. Controlled series compensation for improving the stability of multimachine power systems. IEE Proc C 1995;142:361–6.

[14] Chang J, Chow J. Time optimal series capacitor control for damping inter-area modes in interconnected power systems. IEEE Trans PWRS 1997;12(1):215–21.

[15] Lie T, Shrestha G, Ghosh A. Design and application of fuzzy logic control scheme for transient stability enhancement in power systems. Electric Power Syst Res 1995:17–23.

[16] Wang Y, Mohler R, Spee R, Mittelstadt W. Variable structure FACTS controllers for power system transient stability. IEEE Trans PWRS 1992;7:307–13.

[17] Luor T, Hsu Y. Design of an output feedback variable structure thyristor controlled series compensator for improving power system stability. Electric Power Syst Res 1998;47:71–7.

[18] Rajkumar V, Mohler R. Bilinear generalized predictive control using the thyristor controlled series capacitor. IEEE Trans PWRS 1994;9(4):1987–93.

[19] Zhao Q, Jiang J. A TCSC damping controller using robust control theory. Int J Electrical Power and Energy Syst 1998;20(10):25–33.

[20] Dai X, Liu J, Tang Y, Li N, Chen H. Neural network $\alpha$th-order inverse control of thyristor controlled series compensator. Electric Power Syst Res 1998;45:19–27.

[21] Larsen E, Swann D. Applying power system stabilizers. IEEE Trans PAS 1981;100(6):3017–46.

[22] Tse GT, Tso SK. Refinement of conventional PSS design in multimachine system by modal analysis. IEEE Trans PWRS 1993;8(2): 598–605.

[23] Kundur P, Klein M, Rogers GJ, Zywno MS. Application of power system stabilizers for enhancement of overall system stability. IEEE Trans PWRS 1989;4(2):614–26.

[24] Aarts E, Korst J. Simulated annealing and boltzmann machines: a stochastic approach to combinatorial optimization and neural computing. New York: Wiley, 1989.

[25] Metropolis N, Rosenbluth A, Rosenbluth M, Teller A, Teller E. Equation of state calculations by fast computing machines. J Chem Phys 1953;21:1087–92.

[26] Anderson P, Fouad A. Power system control and stability. Ames, IA: Iowa State University Press, 1977.

[27] Yu YN. Electric power system dynamics. New York: Academic Press, 1983.

[28] Abido MA. A novel approach to conventional power system stabilizer design using tabu search. Int J Electrical Power and Energy Syst 1999;21(6):443–54.


[1] The negative value of $R$ stems from deriving of the one-machine-infinite-bus model by dynamic equivalencing of a multimachine system where smaller generators are replaced by equivalent impedances with negative resistances [27].